Available online at www.sciencedirect.com

ScienceDirect

Physics Procedia 48 (2013) 46 – 54

Physics Procedia

The XIII International Conference on the Physics of Non-Crystalline Solids

Conversion from a bio-inert glass to a glass with bio-active layer by heat-treatment in an oxidation atmosphere

Eun-Tae Kang*, Jong-Po Kim

School of Nano & Advanced Materials Engneering, Gyeongsang University, 660-701, Jinju, Korea

Abstract

The surface of iron-bearing bio-inert glasses was modified by heat-treatment in an oxidizing atmosphere near the glass transition temperature. The modified surfaces after 7 days immersion in simulated body fluid (SBF) solution were analyzed by means of micro-Raman spectroscopy, SEM, and EDS. All investigated glasses except for the glass with NC = 2.6 were able to form hyroxycarbonate apatite (HCA) on their surfaces. The thickness of an HCA surface layer increased with decreased oxygen partial pressure. The cross-sectional micrographs were nearly similar to the 45S5 Bioglass®.

Selection and peer-review under responsibility of Prof. Xiujian Zhao, Wuhan University of Technology

Keyword: Bioglass; Redox; Bio-active glass surface; Iron-bearing glass; Heat treatment

1. Introduction

Bioactive glasses bond to soft tissues as well as bone. The common characteristic of all known bioactive materials is the presence of hydroxycarbonate apatite (HCA) surface layer, which provides the bonding interface with the tissues. A HCA layer on the surface is formed by a sequence of reactions between the bioactive glasses and the surrounding tissues. The bioactive glasses degrade easily according to the reaction mechanism proposed by Hench et al. [1]. Elgayar et al. [2] confirmed that the bioactive glasses are predominantly Q^2 in structure by using ^{29}Si MAS NMR. Thus the compositions of the bioactive glasses are

* Corresponding author. Tel.: +82-55-772-1681; fax: +82-55-772-1689.
E-mail address: etkang@gnu.ac.kr.

Selection and peer-review under responsibility of Prof. Xiujian Zhao, Wuhan University of Technology
doi:10.1016/j.phpro.2013.07.008

limited below 50 mol% SiO_2, which is typical of invert glasses. Many bioactive glasses are based upon the formula called "45S5," signifying 45 wt% SiO_2.

But these glasses have poor chemical durability and strength despite its excellent in vitro and in vivo bioactivity. To enhance the formation of HCA layer, 45S5 Bioglass® includes 6 wt% P_2O_5. However, because the addition of P_2O_5 to the soda lime silicate glasses can cause phase-separations in glasses [3,4], it is difficult to control the reactivity of the glass by altering its composition. One way to avoid these problems is to induce the formation of invert glasses on the surface of the soda lime silicate glasses which don't contain phosphate.

The glass surface can be modified by redox reactions. Many studies on iron-bearing silicate glasses [5-10] showed that heat-treatment of the glasses in an oxidizing atmosphere results in diffusion of mobile network-modifying divalent cations from the interior towards the surface of the glass due to the oxidation of Fe^{2+}. The studies propounded a mechanism of oxidation during which oxidation of the glass occurs not by the diffusive addition of oxygen to the glass, but rather by the diffusive removal of network-modifying cations that is charge compensated by an inward flux of electron holes. Kohlstedt et al. [11] also showed that oxidation occurs internally by the removal of cations rather than by the addition of oxygen in iron-bearing crystalline oxides. Consequently, the surface composition of glass can be modified via oxidation.

It is well known that the composition of bio-active glass is nearly fixed and its behaviors, except for the bioactivity, are intrinsically very poor. Therefore, surface modification of glasses, showing good physical properties, to the composition of the bio-active glass, should be the key to enhancing the other physical properties of glass, together with its excellent bio-activity. The objective of this study is to induce the formation of a bioactive surface layer by treatment of bio-inert glasses under the oxidizing atmosphere at temperature near the glass transition temperature. Specifically, our concern is to consider the effect of oxygen partial pressure on the modification of iron-containing bio-inert glass into the bio-active surface, using heat-treatment.

2. Experimental

Non-bioactive soda-lime silicate glasses were melted in a platinum crucible at 1450℃ for approximately 3 h using a mixture of reagent grade Na_2CO_3, $CaCO_3$, $Fe(C_2O_4)2H_2O$ and sand. Each melt was quenched by pouring it into a cylindrical graphite mold, which was annealed for about 2 h at 400 ℃. Circular glass samples (diameter 14 mm, thickness 2 mm) were prepared by cutting the glass cylinder using a diamond saw. The samples were ground and polished using 1 μm ceria at the final step for XPS analysis. One surface of the samples, used to evaluate bioactivity, was ground with #400 SiC–paper, to increase area exposed to SBF. The glass composition in Table 1 and elsewhere in the present paper is the batch composition in mol%. 45S5 Bioglass® as the reference glass was produced also in the same manner.

The glass transition temperature (T_g) was measured from the onset temperature of the endotherm using differential thermal analysis (DTA)

The oxidation treatment was conducted in an electric furnace under a flow of O_2 or O_2/N_2 gas. The glass samples were inserted into the cold furnace and the gas-flow was turned on. Heating and cooling were conducted with 10 K/min.

Table 1. Composition (mol %), T_g and *NC* of the investigated glasses

Label	SiO_2	CaO	Na_2O	FeO	T_g (℃)	*NC*
M1	54	30	15	1	586	2.30
M2	58	27.33	13.67	1	591	2.55
M3	59	26.67	13.33	1	598	2.61
M4	60	26	13	1	587	2.67

The oxygen partial pressure in the furnace was monitored via a flow-through stabilized zirconia solid-electrolyte sensor that operates at 750℃ in a separate furnace downstream of the reaction furnace. The glasses were treated at near their T_g for 10 h. Simulated body fluid was prepared according to Kokubo and Takadama [12]. The samples heated under oxygen atmosphere were immersed in this solution in sealed containers for the predetermined times and were mechanically agitated at 45 rpm using an incubator set to 36.5℃. After 7 days immersion in SBF the samples were removed and rinsed with distilled water and acetone to remove any residuals salts and halt reactions. The samples were then dried at 60℃ overnight and stored in a vacuum desiccator until required.

The Raman measurements were performed on a Labram HR800 micro-Raman spectrometer in the backscattering geometry. The excitation line was provided by a 17 mW Ar ion laser at 514 nm focused into a 2 ㎛ spot on the sample surface. All spectra were collected with a microscope equipped with lenses 100× and two accumulations at 60 s integration time and a resolution of 2 cm^{-1}.

X-ray photoelectron spectroscopy (XPS) measurements were performed on a Thermo K-alpha XPS spectrometer with a hemispherical analyzer. Spectra were obtained by using monochromatic Al Kα radiation source operated at 72 W. Neutralization of the surface charge was performed by using a low energy flood gun (electrons in the ranges 0-14 eV). The shift of the binding energy due to surface charging effect was calibrated by assuming binding energy of C 1s to be always 284.6 eV. Depth profiles were recorded using the argon ion beam with an energy of 1 keV and a current density of 2 μA/cm^2. The milling rate of the surface was about 216 nm/min. This rate was approximated using a stylus profilometer on the assumption that the milling rate stayed constant throughout the milling process.

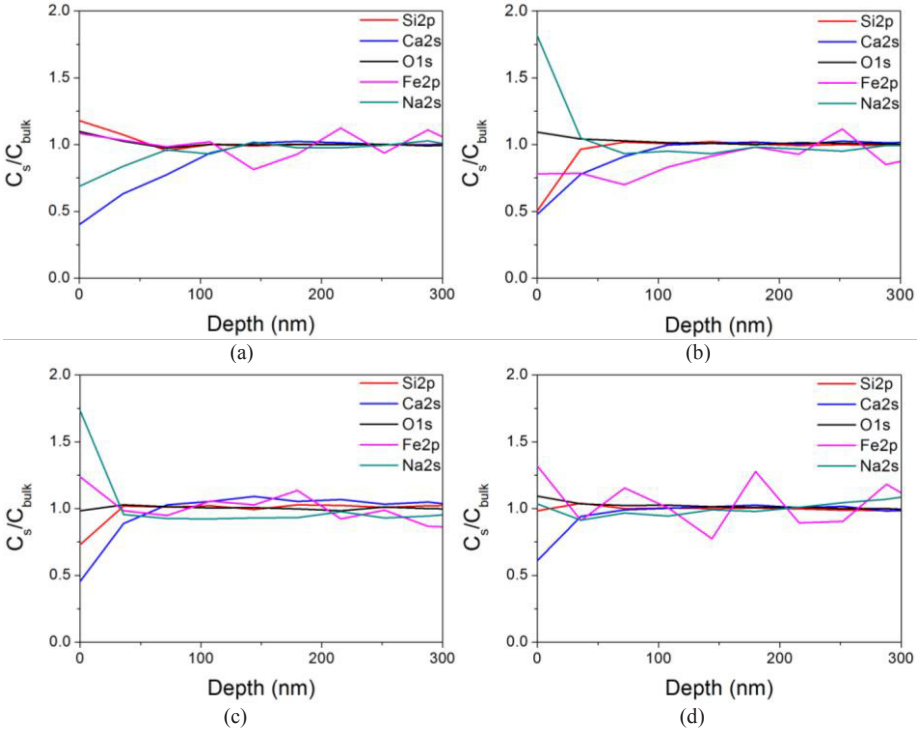

Fig. 1. XPS depth profiles of the M1 glass (a) untreated and heat-treated at 620℃ for 10h in (b) 0.05 atm, (c) 0.21 atm, and (d) 0.36 atm.

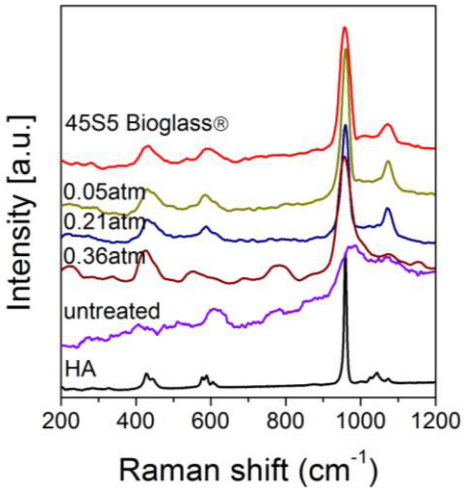

Fig. 2. Raman spectra of M1 glass heat-treated at 620℃ for 10h in various atmospheres and then immersed in SBF solution for 7days

3. Results and Discussion

Fig. 1 shows XPS depth profiles of M1 glass heat-treated at 620℃ for 10h in various oxidizing atmospheres. An enrichment of sodium was observed in approximately the 50 nm surface layer for the heat-treated glasses, as compared with the untreated glass. This result represents that cations acting as charge compensators for ferric iron is the sodium ion, unlike the reported results that primarily the divalent cations diffuse during oxidation of a Fe^{2+}-containing alkali-free glasses [7, 8] or low alkali glasses [5,6,9].

The reason is clarified here but it regards as mainly due to the differences of Na^{+} ion content between the studied glasses. The higher the oxygen partial pressure is, the less the relative concentration of sodium in the surface layer is. This agrees well with a fact [13] that the sodium diffusivity decreases with the $[Fe^{3+}/[Fe]_{tot}$ ratio. Whereas a little depletion of silicon caused by the outward diffusion of sodium was observed near the surface, there was no variation of the calcium content near the surface during the heat treatment in the oxygen atmosphere. Iron profiles are not important here, because the content of iron was very low. However the formation of a sodium-rich surface layer after the heat-treatment in oxidizing atmosphere is significant. This means that the surface of the glasses can be modified into the sodium-rich layer by heat-treatment in an oxidizing atmosphere. The diffusion depth (~50 nm) of the sodium ions was more shallow than that (~200 nm) of alkaline earth ions reported [9]. This can be explained as follows. Since alkali ions are only capable of neutralizing one electron-hole, compared to two holes for alkaline earth ions, the alkali ions are able to carry less positive charges than the alkaline earth ions to charge-balance the flux of electron holes. Also the electron hole motion is much faster than that of both alkali and alkaline earth ions in glasses. Thus the diffusion depth of alkali ions is shorter than that of alkaline earth ions.

Fig. 2 shows Raman spectra of M1 glass heat-treated at 620℃ for 10h in various atmospheres and then immersed in SBF solution for 7days. For comparison purposes, the spectra of hydroxyapatite and 45S5 Bioglass® immersed in SBF for 7days showed as well. The spectra of the samples and 45S5 Bioglass® after immersion in SBF showed very similar results to that of commercial hydroxyapatite.

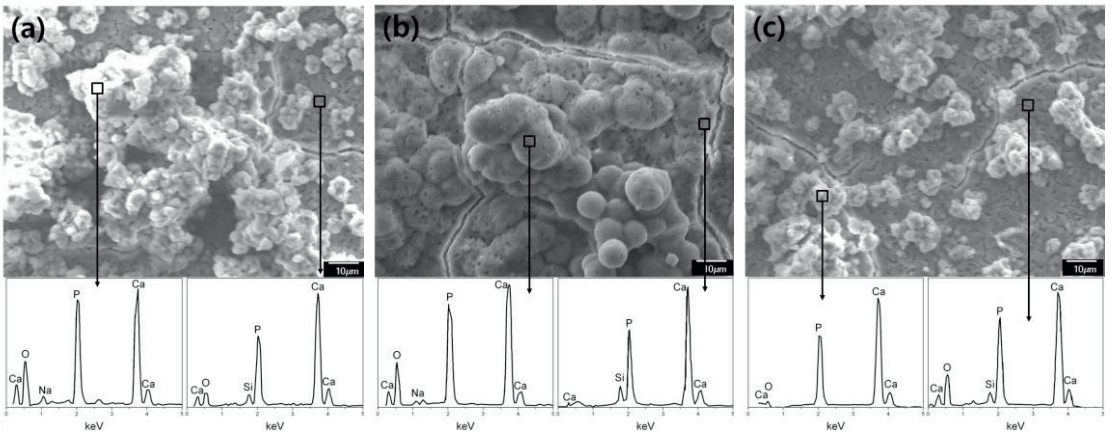

Fig. 3. SEM micrographs and EDS analysis of the M1 glass heat-treated at 620℃ for 10h and then immersed in SBF for 7days: (a) 0.05 atm, (b) 0.21 atm, (c) 0.36 atm.

The highest peak in the spectra is present at 960 cm^{-1} same as for hydroxyapatite. This peak corresponds to the P-O symmetrical confirmed by the weaker peaks corresponding to asymmetrical bending at 438, 454, 580 cm^{-1}. In particular the P–O bend at around 580 cm^{-1} shows the characteristic splitting indicative of crystalline apatite formation [18] into bands at 560 and 600 cm^{-1} as the oxygen partial pressure was lowered. Moreover a peak at about 1070 cm^{-1} associated with a carbonate group [16, 17] appears. The appearance of carbonate bands on exposure to SBF is evidence of crystalline hydroxylcarbonate apatite formation. This discriminates between hydroxyapatite and HCA in the Raman spectra. It is clear that the surface-modified glasses form an HCA surface layer after immersion in SBF. Whereas the spectrum of the untreated M1 glass after 7days immersion in SBF does not show the formation of HCA phase. This indicates that the formation of HCA is possible only when the glasses are heated at near T_g in an oxidizing atmosphere.

Fig. 3 shows SEM micrographs of the surface of the heat-treated M1 glass after 7days of immersion in SBF. It is evident that the main constituent of the surface layer is a large number of droplets, embedded in a continuous matrix. Fig. 3 shows also the EDS analysis which reveal that the droplets are spherical Ca-P particles and the main components of the matrix are also Ca and P. But Si detected in the matrix due to silica gel layer underneath the HCA precipitates. As seen in Fig. 3, Ca-P continuously phase precipitates on the prior layer formed. The Ca/P ratios were less than the ratio (~1.67 [18]) of stoichiometric hydroxyapatite, which is rather small for the first formed layer. This indicates that the composition of hydroxyapatite approaches to stoichiometric composition as the reaction time in SBF increases.. But the CaP layer corresponds to a nonstoichiometric hydroxyapatite containing carbonates like the natural bone as seen from the Raman result.

Fig. 4 shows the SEM microphotographs and EDS elemental mappings of cross-sections of the oxidized M1 glasses after 7days immersion in SBF. It is evident that the microphotographs of the cross-sections can be separated into the three regions in spite of the different oxygen partial pressure, except for the resin layer of the surface. The EDS single element distribution maps of the cross-section reveal that the main components of the outmost layer are Ca and P. If this result is combined with the results of Raman and the ESD analysis of the surfaces, the CaP layer will be a crystalline HCA layer. The thicknesses of HCA layer is between 7.7 ㎛ - 12.7 ㎛, depending on the oxygen partial pressure as shown in Table 2 for M1 glass after 7 days immersion in SBF. The effect of the oxygen partial pressure on the thickness of the HCA layer can be explained by the which the driving force of the diffusion of sodium ions towards the surface is the oxidation of Fe^{2+}.

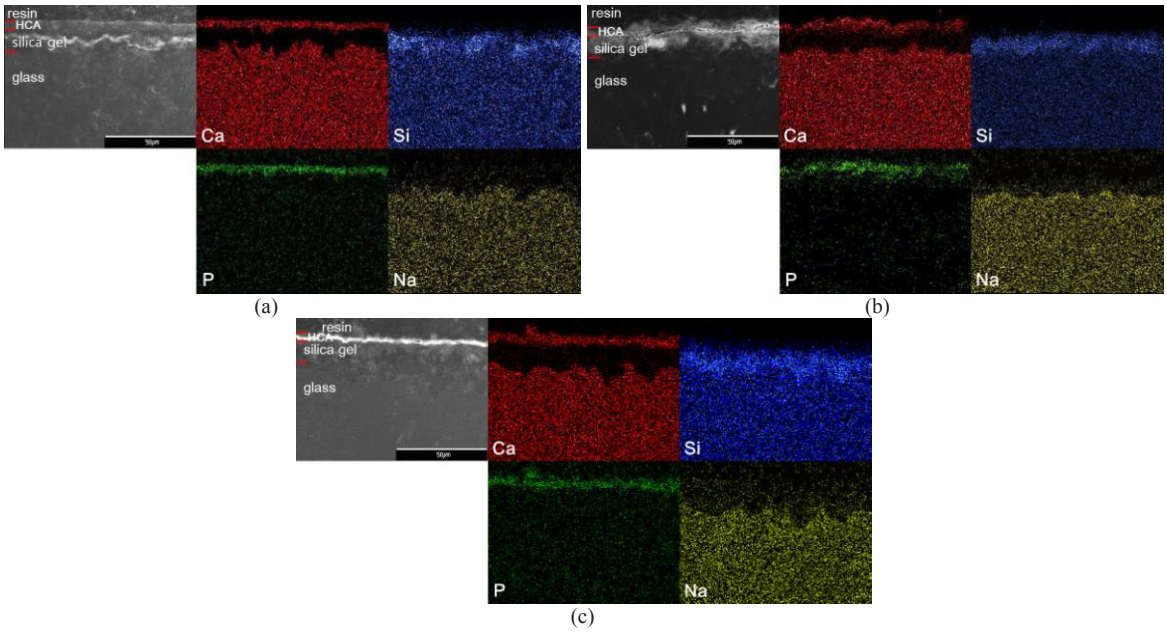

Fig. 4. SEM microphotographs and EDS elemental mappings of cross-sections of the oxidized M1 glasses after 7days immersed in SBF: (a) 0.05 atm, (b) 0.21 atm, (c) 0.36 atm. The scale bars in (a), (b) and (c) are 50 μm.

The concentration of sodium increases, as seen in Fig. 1, as the oxygen partial pressure decreases. This cause to occur easily three reaction stages (ion exchange, hydrolysis of network, polycondensation of silanol of five stages [19-21] leading to the HCA layer formation on the surfaces of the glasses. If the oxygen pressure is too high, all Fe^{2+} ions are oxidized entirely before the mobile ions start to diffuse. Hence, by lowering the oxygen partial pressure, sodium ions diffuse more. This contributes to the thick HCA layer with the reaction in SBF.

The layer underneath the HCA layer shows a high Si content which confirms the presence of a silica-gel layer on the glass surface. In the bottom part, the presence of Si, Ca, Na, Fe, and O is observed which corresponds to the glass composition. Cross-sectional microstructure of the M1 glass after immersion in SBF is nearly similar with that [22] of 45S5 Bioglass®. These results lead to the conclusion that the thickness of the HCA layer increases with the decrease of the oxygen partial pressure.

Certain network connectivity (NC) approaches can be applied to predict the bioactivity of bioglass. The original network connectivity approach taken by Hill [23] recommended an NC close to 2.0 for the ability of bioglass to form apatite. NC is the average number of bridging oxygens per network forming element in the glass structure. The modified NC model (split network model) that accounts for the effect of phosphate contents used by Edén [24] recommends an NC range between 2.0 and 2.6 for optimal bioactivity. It is well known that phosphate plays a key role in bioactivity and apatite formation of bioglass [25-29] and the bioactivity of glasses decreases with the increase of NC [25]. As the glasses under investigation didn't contain phosphate, the original NC approach by Hill applied. As shown in Table 1, NC increases with increasing SiO_2 content. Fig. 5 shows that iron-containing glasses, heat-treated in oxygen partial pressure of 0.05 atm, form the hydroxycarbonate apatite in spite of NC > 2.0, except for M4 glass with high value of NC (2.6). This suggests that the P-free and Fe-bearing glasses with NC < 2.6 can be modified into bio-active glass by heat treating in an oxidizing atmosphere around T_g. As the SiO_2 content increases, the thickness of HCA layer decreases as seen in Table 2. Also Table 2 indicates that the HCA layers formed on the surface of M2 and M3

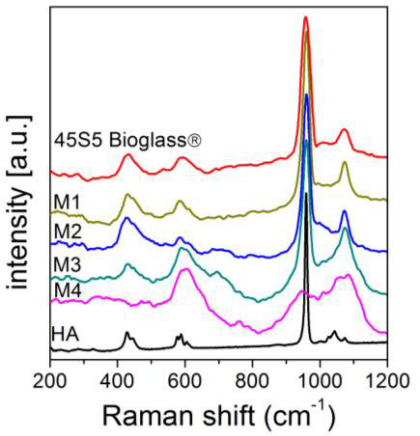

Fig. 5. Raman spectra of the investigated glasses heat-treated at near T_g for 10h in various atmospheres and then immersed in SBF solution for 7days.

glasses are heterogeneous because the uncertainties in thicknesses of these glasses at 95% confidence level are higher than those of the other samples.

Table 2. The thickness of HCA layer formed on the surface after 7days immersion in SBF.

Sample	HCA thickness(μm)
M1, 0.05atm	12.7±0.7
M1, 0.21atm	8.1±0.1
M1, 0.36atm	7.7±0.3
M2	6.1±0.9
M3	4.4±1.0
M4	0

4. Conclusion

The surface of P-free and iron-bearing glass having NC ≥ 2.3 has been modified to a sodium-rich layer by heat-treatment in an oxidizing atmosphere near the glass transition temperature. These glasses are able to form up to 12.7 μm of HCA after 7 days immersion in SBF solution. The thickness of an HCA surface layer increased with decreased the oxygen partial pressure. The HCA layer became heterogeneous as SiO_2 contents increased. The cross-sectional micrographs were nearly similar to those of the 45S5 Bioglass®.

Acknowledgements

This research was supported by Basic Science Research Program through the National Research Foundation of Korea (NRF) funded by the Ministry of Education, Science and Technology (No. 2010-0021047).

References

[1] Hench, L.L., Splinter, R.J., Allen, W.C., and Greenlee, Jr. T.K., 1971, Bonding mechanism at the interface of ceramics prosthetic materials, J Biomed Mater Res. 2(1), p. 117.
[2] Elgayar, I., Aliev, A.E., Boccaccini, A.R., and Hill, R.G., 2005, Structural analysis of bioactive glasses, J Non-Cryst Solids, 351, p. 173.
[3] Tilocca, A. and Cormack, A.N., 2007, Structural effects of phosphorus inclusion in bioactive silicate glasses, J Phys Chem., B111 (51), p. 14256.
[4] O'Donnell, M.D., Watts, S.J., Law, R.V. and Hill, R.G., 2008, Effect of P_2O_5 content in two series of soda lime phosphosilicate glasses on structure and properties – Part I: NMR, J Non-Cryst Solids, 354, p. 3554.
[5] Cook, G.B., Cooper, R.F. and Wu, T., 1990, Chemical diffusion and crystalline nucleation during oxidation of ferrous iron-bearing magnesium aluminosilicate glass, J. Non-cryst. Solids, 120, p. 207.
[6] Cooper, R.F., Fanselow, J.B. and Poker, D.B., 1996, The mechanism of oxidation of a basaltic glass:Chemical diffusion of network-modifying cations, Geochim. Cosmochim. Acta, 60, p. 3253.
[7] Smith, D.R. and Cooper, R.F., 2000, Dynamic oxidation of a Fe^{2+}-bearing calcium–magnesium–aluminosilicate glass: the effect of molecular structure on chemical diffusion and reaction morphology, J. Non-cryst. Solids, 278, p. 145.
[8] Cook, G.B. and Cooper, R.F., 2000, Iron concentration & the physical processes of dynamic oxidation in an alkaline earth aluminosilicate glass, Am. Mineral., 85, p. 397.
[9] Smedskjaer, M.M. and Yue, Y.Z., 2011, Inward and Outward Diffusion of Modifying Ions and its Impact on the Properties of Glasses and Glass–Ceramics, Innternational J. Applied Glass Science, 2, p. 117.
[10] Magnien, V., Neuville, D.R., Cormier, L., Roux, J., Hazemann, J.-L., de Ligny, D., Pascarelli, S., Vickridge, I., Pinet, O., Richet, P., 2008, Kinetics and mechanisms of iron redox reactions in silicate melts: The effects of temperature and alkali cations, Geochim. Cosmochim. Acta, 72, p. 2157.
[11] Wu, D. and Kohlstedt, D.L., 1988, A Rutherford backscattering spectroscopy study of the kinetics of oxidation of $(Mg,Fe)_2SiO_4$., J Am Ceram Soc., 71(7), p. 540.
[12] Kokubo, T. and Takadama, H., 2006, How useful is SBF in predicting in vivo bone bioactivity?, Biomaterials, 27, p. 2907.
[13] Smedskjaer, M.M., Zheng, Q.J., Mauro, J.C., Potuzak, M., Mørup, S. and Yue, Y.Z., 2011, Sodium diffusion in boroaluminosilicate glasses, J. Non-Cryst. Solids, 357, p. 3744.
[14] Antonakosa, A., Liarokapisa, E. and Leventouri, T., 2007, Micro-Raman and FTIR studies of synthetic and natural apatites, Biomaterials, 28, p. 3043.
[15] Penel, G., Leroy, G., Rey, C., Sombret, B., Huvenne, J.P., Bres, E., 1997, On the assessment of hydroxyapatite fluoridation by means of Raman scattering, J Mater Sci Mater Med., 8, p. 271.
[16] Penel, G., Leroy, G., Rey, C. and Bres, E., 1998, MicroRaman Spectral Study of the PO_4 and CO_3 Vibrational Modes in Synthetic and Biological Apatites, Calcif Tissue Int., 63, p. 475.
[17] Awonusi, A., Morris, M.D. and Tecklenburg, M.M.J., 2007, Carbonate assignment and calibration in the Raman spectrum of apatite, Calcif Tissue Int., 81, p. 46.
[18] Liu, H., Yazici, H., Ergun, C., Webster, T.J. and Bermek, H., 2008, An in vitro evaluation of the Ca/P ratio for the cytocompatibility of nano-to-micron particulate calcium phosphates for bone regeneration, Acta. Biomater., 4, p. 1472.
[19] Cao, W. and Hench, L.L., 1996, Bioactive Materials, Ceram. Int., 22, p. 493.
[20] Kim, C.Y., Clark, A.E. and Hench, L.L., 1989, Early Stages of Calcium-Phosphate Layer Formation in Bioglasses, J. Non-Cryst. Solids, 113, p. 195.
[21] Rehman, I., Hench, L.L., Bonfield, W. and Smith, R., 1994, Analysis of surface layers on bioactive glasses, Biomaterials, 15, p. 865.
[22] Bellucci, D., Bolelli, G., Cannillo, V., Cattini, A. and Sola, A., 2011, In situ Raman spectroscopy investigation of bioactive glass reactivity: Simulated body fluid solution vs. TRIS-buffered solution, Mater. Character., 62, p. 1021.
[23] Hill, R. G., 1996, An alternative view of the degradation of bioglass, J. Mater. Sci. Lett., 15, p. 1122.
[24] Edén, M., 2011, The split network analysis for exploring composition – structure correlations in multi-component glasses: I. Rationalizing bioactivity-composition trends of bioglasses, J. Non-Cryst. Solids, 357, p. 1595.

[25] Hill, R. G. and Brauer, D. S., 2011, Predicting the bioactivity of glasses using the network connectivity or split network models, J. Non-Cryst. Solids, 357, p. 3884.
[26] O'Donnell, M.D., Watts, S.J., Hill, R.G. and Law, R.V., 2009, The effect of phosphate content on the bioactivity of soda-lime-phosphosilicate glasses, J. Mater. Sci.: Mater. Med., 20, p. 1611.
[27] Tilocca, A. and Cormack., A.N., 2007, Structural Effects of Phosphorus Inclusion in Bioactive Silicate Glasses, J. Phys. Chem., 111, p. 14256.